Journal of Ceramic Processing Research. Vol. 7, No. 3, pp. 224~229 (2006)

J O U R N A L O F
Ceramic Processing Research

Fabrication of ultrafine binderless WC and WC-Ni hard materials by a pulsed current activated sintering method

Hwan-Cheol Kim, In-Jin Shon*, In-Yong Ko, Jin-Kook Yoon[a], Jung-Mann Doh[a] and Gyu-Won Lee[b]

Department of Advanced Materials Engineering, The Research Center of Advanced Materials Development, Chonbuk National University, Jeonbuk 560-756, Korea

[a]Metal Processing Research Center, Korea Institute of Science and Technology, P.O. Box 131, Cheongryang, Seoul 136-791, Korea

[b]Department of Civil Engineering, The Research Center of Industrial Technology, Engineering Research Institute, Chonbuk National University, Jeonbuk 560-756, Korea

Using a pulsed current activated sintering (PCAS) method, the densification of binderless WC and WC-Ni hard materials were accomplished using ultra fine powder of Ni and WC. The advantage of this process is that it allows very quick densification to near theoretical density and the prohibition of grain growth in nano-structured materials. Nearly fully dense WC and WC-Ni with a relative density of up to 97.6% could be obtained with the simultaneous application of 60 MPa pressure and electric current within 2 minutes without a significant change in grain size. The average grain size of WC was about 350 nm The hardness, fracture toughness, and the relative densities of the dense WC and WC–*x*wt.%Ni (x=8, 10, 12) composites produced by PCAS were investigated.

Key words: Rapid Sintering, Pulsed Current Activated Sintering, WC-Ni composites, Hard Materials, Hardness, Fracture Toughness.

Introduction

Many of the transition metal carbides (e.g., WC, TaC, and TiC) are high melting-temperature compounds with high hardness, high thermal and electrical conductivities, and a relatively high chemical stability. They are primarily used as cutting tool and abrasive materials in single-phase and composite structures. In the latter case, their use as cemented carbides (particularly WC) involves the formation of a composite with a binder metal, such as Co or Ni. Tungsten carbide has a high melting point (a peritectic melting temperature of 2785°C) and high hardness (16-26 GPa Vickers) [1-3]. In addition to its use as a cutting material, it has been considered for other uses such as a catalyst (substituting for noble metals) [4-6], as a catalyst electrode in fuel cells, and as a coating for aerospace components [7].

Most cemented carbides of tungsten utilize cobalt as the binder. But the high cost of cobalt and the low corrosion resistance of the WC-Co cermet [8] have prompted considerable research effort aimed at finding a satisfactory alternative binder phase [9-11]. It has been shown that by using Ni instead of Co, the corrosion and oxidation resistance of the resulting cermet is improved [8] but the mechanical properties (hardness and toughness) are somewhat lower than those of WC-Co [9].

Additionally, property improvements can be obtained through microstructural changes, notably by grain size refinement [12, 13]. However, preparation and processing of cemented carbides having a refined grain structure can result in residual porosity attributed to localized agglomeration of the powders [14]. Moreover, the use of conventional methods to consolidate nano-powders often results in grain growth [15]. Minimization of grain growth can be achieved if sintering can be carried out at lower temperatures and for shorter times. In this regard, the spark plasma sintering (SPS) method has been shown to be effective in achieving this goal [16, 17]. Also recently the high-frequency induction-heated sintering (HFIHS) technique has been shown to be effective in the sintering of nanostructured materials in very short times (within 1 minute) [18, 19]. When a high pressure is applied, the contribution of plastic yielding to densification is such that lower temperatures and shorter times are required for the overall compaction process.

In this paper, we report results on the sintering of binderless WC and WC-Ni by a rapid sintering process, pulsed current activated sintering (PCAS), a method which combines pulsed current with high-pressure application. The goal of this work is to produce dense,

*Corresponding author:
Tel : +82-63-270-2381
Fax: +82-63-270-2386
E-mail: ijshon@chonbuk.ac.kr

ultra-fine WC-*x*wt.%Ni (*x*=0, 8, 10, 12) hard materials in very short time sintering times (< 2 minutes). Also we investigated the effect of Ni binder on the mechanical properties of WC hard materials.

Experimental Procedure

The tungsten carbide powder used in this research was supplied by TaeguTec Ltd. (Taegu, Korea). The powder had a grain size of 0.4 μm measured by a Fisher sub-sieve sizer (FSSS) and was reported to be 99.5% pure. Nano-sized nickel (60~80 nm), obtained from Inframat, (Farmington, CT, USA) was used as a binder material. Four different compositions were investigated: Binderless WC, WC-8wt.%Ni, WC-10wt.%Ni, and WC-12wt.%Ni. Field-emission scanning electron microscope (FE-SEM) images of the starting powders are shown in Fig. 1. As can be seen from this figure, the WC grains and the Ni grains are generally round and exhibit some agglomeration. All powders were milled in a Universal Mill with a ball-to-powder weight ratio of 6:1. Milling was done in polyethylene bottles using tungsten carbide balls and was performed at a horizontal rotation velocity of 300 rpm for 48 h.

The powders were placed in a graphite die (outside diameter, 45 mm; inside diameter, 20 mm; height, 40 mm) and then introduced into the pulsed-current activated sintering system made by Eltek Co. in the

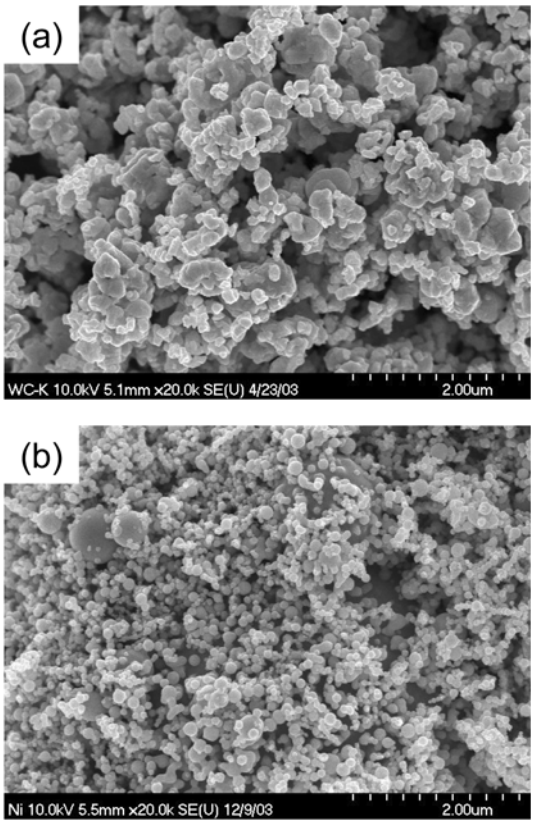

Fig. 1. Field Emission Scanning Electron Microscope images (a) WC and (b) Ni raw materials.

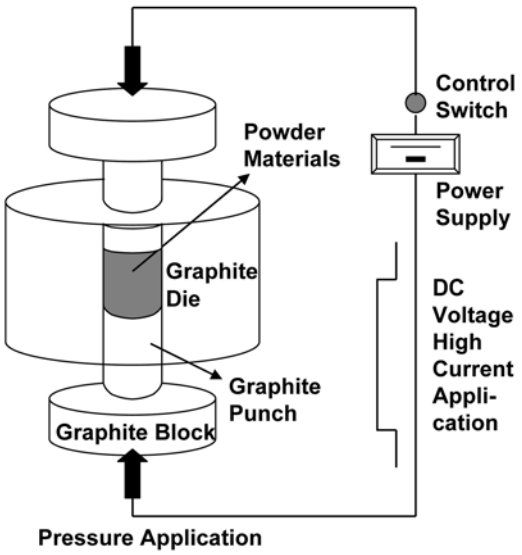

Fig. 2. Schematic diagram of apparatus for pulsed current activated sintering.

Republic of Korea. A schematic diagram of this method is shown in Fig. 2. The PCAS apparatus includes an 18V, 2800A DC power supply (which provides a pulsed current with 20 μsec on time and 10 μsec off time through the sample and die) and a 50 kN uniaxial press. The system was first evacuated and a uniaxial pressure of 60 MPa was applied. A DC current was then activated and maintained until the densification rate was negligible, as indicating by the observed shrinkage of the sample. Sample shrinkage was measured in real time by a linear gauge measuring the vertical displacement. Temperatures were measured by a pyrometer focused on the surface of the graphite die. Depending on heating rate, the electrical and thermal conductivities of the compact, and on its relative density, a difference in temperature between the surface and the center of the sample exists. The heating rates were approximately 1400 °C/min in the process. At the end of the process, the current was turned off and the sample was allowed to cool to room temperature. The entire process of densification using the PCAS technique consists of four major control stages. These are chamber evacuation, pressure application, power application, and cool down. The four major stages in the sintering are shown schematically in Fig. 3. The process was carried out under a vacuum of 5.33 Pa.

The relative densities of the sintered samples were measured by the Archimedes method. Microstructural information was obtained from product samples, which had been polished and etched, using Murakami's reagent (10 g potassium ferricyanide, 10 g sodium hydroxide, and 100 ml water), for 1-2 minutes at room temperature. Compositional and microstructural analyses of the products were made through X-ray diffraction (XRD), scanning electron microscopy (SEM) with energy dispersive spectroscopy (EDS) and field-emission scann-

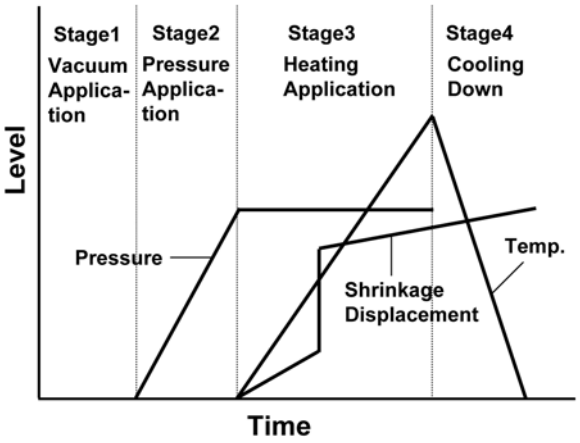

Fig. 3. Schematic representation of the temperature, pressure and shrinkage displacement profiles during PCAS.

ing electron microscopy (FE-SEM). Vickers hardness was measured by performing indentations at a load of 30 kg_f with a dwell time of 15 s. The carbide grain size, d_{wc} was obtained by the linear intercept method [20, 21].

Results and Discussion

Densification Behavior and Microstructure

The variations of shrinkage and temperature with heating time during the sintering of WC-*x*wt.%Ni by PCAS under 60 MPa pressure and pulsed DC current of 2800A are shown in Fig. 4. In the case of binderless WC, initially the sample exhibits an increase in volume due to thermal expansion. As the electric current is applied, the shrinkage displacement increased with temperature up to about 1200°C, and then abruptly increased as the temperature is further increased from this value. When the temperature reaches about 1600 °C, the densification rate becomes nearly negligible, and as will be seen later, the samples have densified to 97.6% of theoretical density in about 110s. In the case of WC-Ni hard materials, as the electric current is applied, the shrinkage displacement increased directly without thermal expansion and variation of the shrinkage displacement with heating temperature was almost similar. When the temperature reaches about 1350 °C, the densification rate of WC-Ni hard materials becomes nearly negligible, and as will be seen later, the samples have densified to 96.5% of theoretical density in about 45s. The densification temperature of WC was reduced remarkably by the addition of Ni. So, it is expected that Ni would be molten during the continuation of the sintering. The main densification mechanism for this is carbide particle rearrangement, enhancement of the diffusion and viscous flow of the binder [22].

The temperature distribution during the PCAS experiment (both within the sample and in the die) is important. Despite its crucial importance, an evaluation of the accuracy of temperature measurement in the PCAS has received relatively little attention. It is common practice to measure and control the temperature during PCAS experiments using an optical pyrometer focused on the external surface of the die. While this may be adequate for very slow heating rates where thermal equilibrium can be attained, it is not satisfactory for high heating rates, whose feasibility is one of the most obvious advantages of the PCAS process. Furthermore, since heating is resistive, the temperatures inside the sample and that on the surface depend on the conductivity of the sample, as well as that of the die. The difference in temperature between the sample and the die surface was shown in Fig. 5. This figure shows two temperature profiles obtained, simultaneously, one by the pyrometer and the other by a thermocouple positioned in contact with the WC-10wt.%Ni sample. At low temperatures (around 600 °C, the lower limit for our optical pyrometer), the difference between both readings is negligible, but it becomes very significant at higher temperatures, being about 300 °C at 1500 °C because of the heat loss of the die surface by radiation or convection of heat.

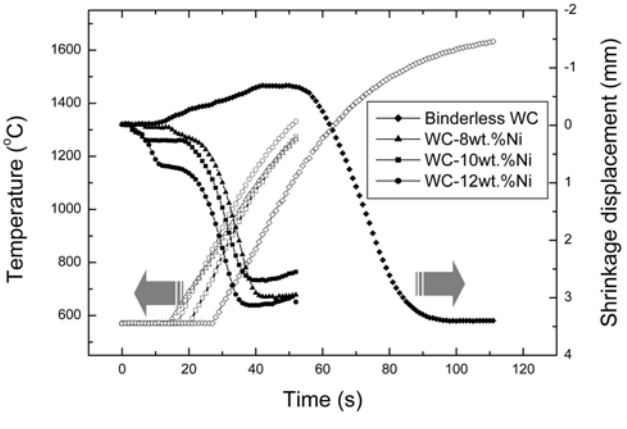

Fig. 4. Variations of temperature and shrinkage displacement with heating time during PCAS of WC-Ni hard materials.

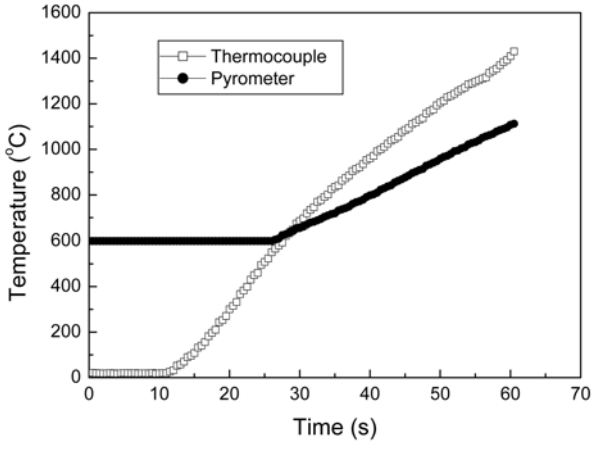

Fig. 5. Difference of temperature between specimen and die surface of WC-10wt.%Ni in PCAS.

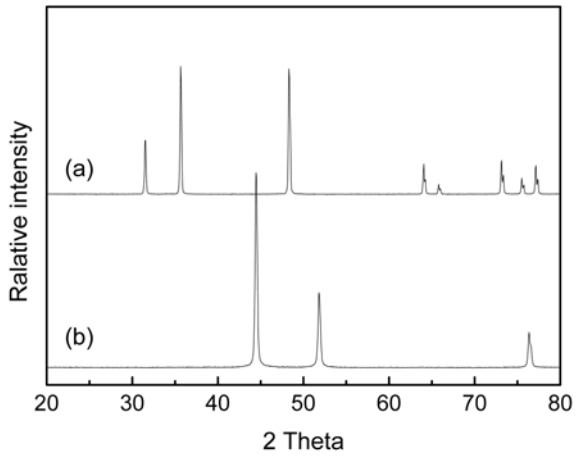

Fig. 6. XRD patterns of raw materials (a) WC and (b) Ni.

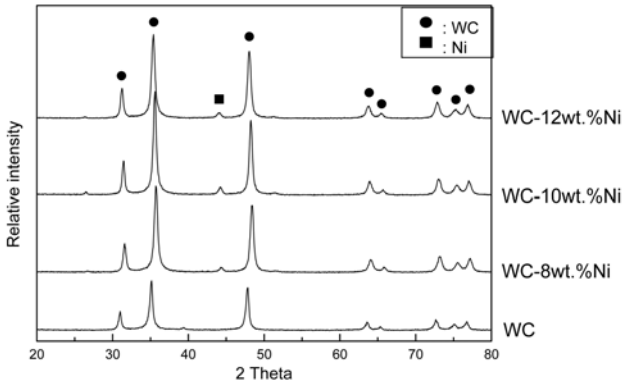

Fig. 7. XRD patterns of WC-Ni hard materials produced by PCAS.

Figure 6 shows the X-ray diffraction patterns of the raw materials used and Fig. 7 shows the XRD patterns of WC and WC-Ni composites after sintering by the PCAS method, respectively. In both cases, only Ni and WC peaks are detected; the intensity of the former slightly increases as its content in the composite increased. No peaks for the sub-carbide W_2C or any impurity phase are present. SEM images of etched surfaces of samples heated to about 1350 °C for the case of WC-Ni and heated to about 1600 °C for the case of binderless WC under a pressure of 60 MPa using the PCAS method are shown in Fig. 8. The initially relatively round WC grains have become faceted during sintering. The faceting reflects the difference in surface energy of the (010) and (100) planes. Because of this anisotropy, WC grains tend to attain a triangular prism shape, as has been observed before [23]. The average size of these grains in all the nearly fully dense WC-*x*wt.%Ni composites, determined by the linear intercept method, is about 350 nm. Thus the fine structure can be obtained without grain growth during the sintering by the PCAS method.

The dependence of WC grain size and relative density of the WC-Ni cermets on Ni content for samples produced by the PCAS is shown in Fig. 9. The grain

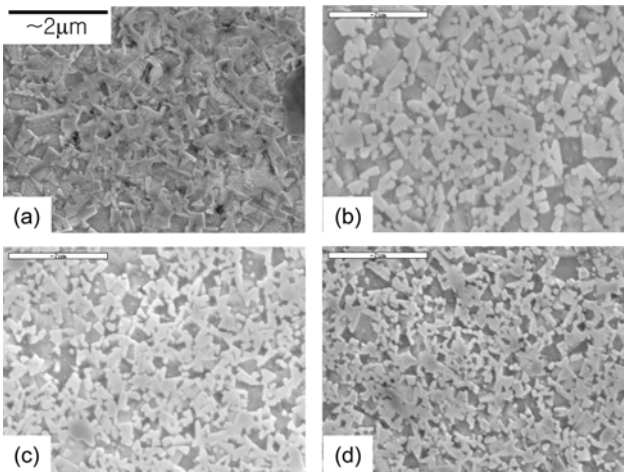

Fig. 8. Scanning Electron Microscope images of WC and WC-Ni hard materials produced by PCAS (a) WC, (b) WC-8wt.%Ni, (c) WC-10wt.%Ni (d) WC-12wt.%Ni.

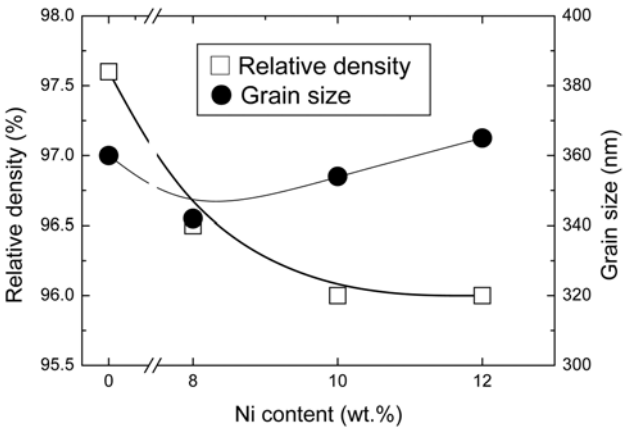

Fig. 9. Relative density and grain size as a function of Ni content in WC-Ni hard materials.

sizes of WC for all cases of WC-xwt.%Ni(x=0, 8, 10, 12) are similar. The relative densities of binderless WC, WC-8wt.%Ni, WC-10wt.%Ni and WC-12wt.%Ni hard materials were about 97.6%, 96.5% 96.0% and 96.1%, respectively. The attainment of a higher density and a finer structure in a short time using electric heating with a pressure is not well understood. However, we would suggest that the accelerated PCAS densification may be attributed to a combination of electrical discharge, resistance heating, and pressure application effects. When the electric current is applied, energy emission may be concentrated at particle contacts that attain high temperatures. These concentrated heat effects at particle surfaces may cause surface melting and oxide breakdown, similar to surface effects in the electrodischarge machining (EDM) process [24].

Physical and Mechanical Properties

Vickers hardness measurements were made on polished sections of the binderless WC and WC-Ni composites using a 30 kg_f load and a 15 s dwell time. Indentations

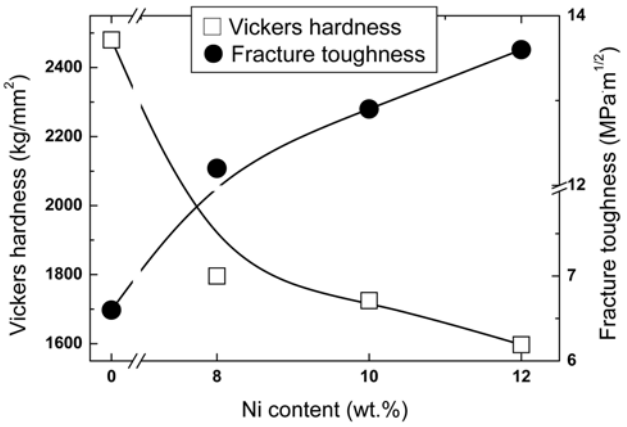

Fig. 10. Vickers hardness and fracture toughness as a function of Ni content in WC and WC-Ni hard materials.

with large enough loads produced radial cracks emanating form the corners of the indent. The length of these cracks permits an estimation of the fracture toughness of the material by means of the Anstis expression [25].

$$K_{IC} = 0.016(E/H)^{1/2}\ P/C^{3/2} \quad (1)$$

where E is Young's modulus, H the indentation hardness, P the indentation load, and C the trace length of the crack measured from the center of the indentation. Typically, one to three additional cracks were observed to propagate radially from the indentation. As in the case of hardness values, the toughness values are derived from the average of ten measurements. The calculated hardness value and fracture toughness value of binderless WC and WC-Ni composites are shown in Fig. 10 as a function of Ni content for samples produced PCAS. As expected, the Vickers hardness decreased and the fracture toughness increased with increasing Ni content.

In Table 1, we provide a comparison of the hardness and fracture toughness values obtained in this work with those reported by others [9, 18]. In one of the reported studies [9], WC-Co and WC-Ni were sintered at 1380 and 1420 °C by conventional methods. The mechanical properties of WC-Co composite are higher than those of the WC-Ni composite. Referring to Table 1, it is seen that refinement of the WC grain size significantly improves the hardness of cemented WC without decreasing the fracture toughness. The hardness of the binderless WC samples made in this study is the highest. Also comparing this investigation (WC-10Ni) with a study of WC-10 Co [18], there is a little difference in hardness due to the decrease of relative density with the same fracture toughness.

Table 1. Comparison of mechanical properties of WC-Ni sintered in this study with previously reported values

Ref.	Binder content (wt%)	Relative density (%)	Grain size (μm)	Hv (kg/mm²)	K_{IC} (MPa·m$^{1/2}$)
9	10 Co	99.5	1.9	1333	13.5
9	9.6Ni-0.4Co	99.5	1.8	1180	12.5
18	10 Co	99.5	0.26	1886	13
This work	10 Ni	96.5	0.35	1720	12.9
	WC	97.6	0.36	2480	6.6

Summary

Using pulsed current activated sintering, the rapid consolidation of binderless WC and WC-Ni hard materials were accomplished using ultra fine powder of Ni and WC. Nearly fully dense WC and WC-Ni could be obtained within 2 minutes. The densification temperature of WC was reduced remarkably by the addition of Ni. The grain size of WC was about 350 nm. The fracture toughness and hardness values of WC, WC-8Ni, WC-10Ni, and WC-12Ni made by PCAS were 6.6 MPa·m$^{1/2}$ and 2480 kg/mm^2, 12.2 MPa·m$^{1/2}$ and 1796 kg/mm^2, 12.9 MPa·m$^{1/2}$ and 1725 kg/mm^2, 13.6 MPa·m$^{1/2}$ and 1597 kg/mm^2, respectively for 60 MPa and a pulsed DC current of 2800A. The mechanical properties of WC-Ni obtained by PCAS were higher than those obtained by a conventional method.

Acknowledgements

This study was supported by a grant from the Center for Advanced Materials Processing (CAMP) of the 21th Century Frontier R&D program funded by the Ministry of Commerce, Industry and Energy (MOCIE), Republic of Korea, and Jung-Won Engineering Co., Ltd. in Korea.

References

1. P. Schwartzkopf and R. Kieffer, in "Refractory Hard Metals-Boride, Carbide, Nitride and Silicide" (MacMillan, 1953) p. 1.
2. L.E. Toth, in "Transition Metal Carbides and Nitrides" (Academic Press, 1971) p. 1.
3. H.C. Kim, I.J. Shon, J.E. Garay, and Z.A. Munir, Int. J. of Refract. Met. and Hard Mater. 22 (2004) 257-264.
4. L. Leclercq, M. Provost, H. Pastor, G. Grimblot, A.M. Hardy, and L. Gengembre, J. Catalysis 117 (1989) 371-383.
5. M.J. Ledoux, C.H. Pham, J. Guille, and H. Dunlop, J. Catalysis 134 (1992) 383-398.
6. L. Volpe and M. Boudart, J. Solid State Chem. 59 (1985) 348-356.
7. R. Koc and S.K. Kodambaka, J. Eur. Ceram. Soc. 20 (2000) 1859-1869.
8. S. Imasato, K. Tokumoto, T. Kitada, and S. Sakaguchi, Int. J. of Refract. Met. and Hard Mater. 13 (1995) 305-312.
9. E.A. Almond and B. Roebuck, Mater. Sci. Eng. A105/106 (1988) 237-248.
10. G. Gille, J. Bredthauer, B. Gries, B. Mende, and W. Heinrich, Int. J. of Refract. Met. and Hard Mater. 18 (2000) 87-102.
11. P. Goeuriot and F. Thevenot, Ceramics International 13 (1987) 99-103.

12. H. Gleiter, Progress in Materials Science 33 (1989) 223-315.
13. G.E. Fougere, J.R. Weertman, R.W. Siegel, and S. Kim, Scripta Metallurgica et Materialia 26 (1992) 1879-1883.
14. T.S. Srivatsan, R. Woods, M. Petraroli, and T.S. Sudarshan, Powder Technology 122 (2002) 54-60.
15. R.B. Schwarz, S.R. Srinivasan, J.J. Petrovic, and C.J. Maggiore, Mater. Sci. Eng. A155 (1992) 75-83.
16. M. Omori, Mater. Sci. Eng. A287 (2000) 183-188.
17. S.I. Cha and S.H. Hong, Mater. Sci. Eng. A356 (2003) 381-389.
18. H.C. Kim, I.J. Shon, and Z.A. Munir, J. Mater. Sci. 40 (2005) 2849-2854.
19. H.C. Kim, D.Y. Oh, and I.J. Shon, Int. J. of Refract. Met. and Hard Mater. 22 (2004) 197-203.
20. K. Jia, T.E. Fischer, and G. Gallois, Nanostruct. Mater. 10 (1998) 875-891.
21. J.H. Han and D.Y. Kim, Acta Mater. 46 (1998) 2021-2028.
22. G.S. Upadhyaya, Materials & Design 22 (2001) 483-489.
24. A.V. Shatov, S.A. Firstov, and I.V. Shatova, Mater. Sci. Eng. A242 (1998) 7-14.
24. J. Fleischer, T. Masuzawa, J. Schmidt, and M. Knoll, J. Mater. Proce. Tech. 149 (2004) 246-249.
25. G.R. Anstis, P. Chantikul, B.R. Lawn, and D.B. Marshall, J. Am. Ceram. Soc. 64 (1981) 533-538.